

Article

Performance Analysis of a PEMFC-Based Grid-Connected Distributed Generation System

Alper Nabi Akpolat ^{1,*} , Erkan Dursun ¹  and Yongheng Yang ² 

¹ Department of Electrical-Electronics Engineering, Faculty of Technology, Marmara University, Istanbul 34854, Turkey

² College of Electrical Engineering, Zhejiang University, Hangzhou 310027, China

* Correspondence: alper.nabi@marmara.edu.tr; Tel.: +90-216-777-3843

Abstract: Less energy consumption and more efficient use of renewables are among the sustainable energy targets of modern societies. The essential activities to be achieved under these objectives are to increase distributed generation (DG) structures' applicability. DG systems are small-scale versions of the traditional power grid; they are supported by micro turbines, photovoltaics (PV) modules, hydrogen fuel cells, wind turbines, combined heat and power systems, and energy storage units. The aim of this research is to detail the performance analysis of a proton-exchange membrane fuel cell (PEMFC)-based grid-connected distributed generation system with the help of empirical calculations. To this end, we aimed to establish the system and analyze the performance of the reliable operation of the system with experimental verifications. The findings demonstrate how much power can be generated annually, through real meteorological data, to dispatch to constantly variable loads. While 53.56% of the total energy demand is met by the utility grid, 46.44% of the demand is met by the produced energy i.e., from the DG. The PEMFC-based DG system analyzed in detail in this study was located at Marmara University. According to the results of the performance analysis, significant points of this study will be highlighted to assist the researchers working in this field. Our results are encouraging and can be certified by a larger sample size with neat weather conditions in terms of the percentage of procurement of energy.

Keywords: distributed generation (DG); fuel cell; wind turbine; photovoltaic (PV); performance analysis



Citation: Akpolat, A.N.; Dursun, E.; Yang, Y. Performance Analysis of a PEMFC-Based Grid-Connected Distributed Generation System. *Appl. Sci.* **2023**, *13*, 3521. <https://doi.org/10.3390/app13063521>

Academic Editor: Aliaksandr Shaula

Received: 26 January 2023

Revised: 28 February 2023

Accepted: 7 March 2023

Published: 9 March 2023



Copyright: © 2023 by the authors. Licensee MDPI, Basel, Switzerland. This article is an open access article distributed under the terms and conditions of the Creative Commons Attribution (CC BY) license (<https://creativecommons.org/licenses/by/4.0/>).

1. Introduction

All technological developments have emerged in line with specific needs. Scientists, researchers, engineers, and inventors seek solutions to the problems encountered while working on meeting the needs of people. In response to the problems faced by traditional grids, researchers and scientists have agreed on the need for modernization of traditional systems. The main problems encountered in traditional grids are transmission losses and energy security due to the transfer of the generated energy to loads that are kilometers away. According to the U.S. Department of Energy, modular, small-scale, on-grid, or off-grid systems, consisting of wind turbines, photovoltaic (PV) modules, hydrogen fuel cells, and energy storage units that provide near-load installation, are considered distributed generation (DG) systems [1]. DG systems are able to continue operating during blackouts, which allows flexible and efficient electrical energy distribution with an integration of renewable energy. DGs are designed for small and medium-sized electric power grids to provide energy for dynamic load groups such as organized industrial sites, research and development centers, university campuses, and technoparks [2].

Many definitions are used for DG in the literature. The definition of the nominal value of each distributed power station also differs depending on the country. Due to the variations when defining DG, the following parameters must be determined: the power location area, the capacity of DG, the used technology, and the operation mode. DG requires

efficient and cost-effective integration with the existing grid [3]. It can be presumed that the DG is a flexible energy generation system that can operate either connected or independent from the grid, providing installation close to the load groups. This is operated conveniently for flexible and dynamic load groups such as university campuses, educational institutions, and research and development centers. In [4], the design and implementation of a virtual laboratory for microgrids with renewable-based DGs is proposed to realize innovative courses using LabVIEW, Microsoft, and Simulink. That virtual laboratory is presented with the objectives of scalability, interaction, maintainability, and fast response time for a microgrid structure renewable energy sources. Similarly, in [5], lead acid energy storage system technology is used to address cold ambient temperatures using a standalone wind–PV-based DG system. The technical and economic performance of some alternative systems exploiting renewable energy, such as heat pumps and a PV plant, is presented in [6], showing promising energy savings outputs compared to the traditional electrical grids and storage.

In [7], the authors presented the design and implementation of a microgrid teaching laboratory whose structure consists of a wind turbine, PV, battery bank, and DC/DC and DC/AC converters for dispatching the energy from sources and the utility grid to the load side. The design, implementation, and operation of an education laboratory-scale microgrid facilitate the use of renewable energy, which is a crucial improvement in the awareness of green–clean energy technology. Apart from this approach, [8] proposes the implementation of a single-controllable DG structure in the engineering school of the Federal University of Minas Gerais using commercial devices.

Although DGs provide flexibility in energy management, the energy production capacities of the wind turbine and PV modules depends largely on meteorological conditions. Therefore, in the absence of sufficient wind and sun, a third supporting energy generation system is needed. In this study, to use the potential of renewables, a PV, wind, and hydrogen fuel cell energy storage-based hybrid power system is established. The hydrogen fuel cell stack is utilized as a back-up power generation system based on the relevant literature. The hydrogen used by the fuel cell is produced by the electrolyzer operating with the energy produced by renewable energy sources. This ensures a completely clean and sustainable energy conversion [9]. In this study, detailed performance analysis of the proton exchange membrane fuel cell (PEMFC)-based grid-connected DG system is established and analyzed at Marmara University, Faculty of Technology, Istanbul, Turkey.

The rest of the paper is organized as follows: first, DG case studies at different universities are presented in brief. The next section outlines the factors that need to be set up for DG system design in an overview of hybrid microgrid systems. In this section, each component is examined in detail, and its effectiveness is evaluated. The next section provides discussion points on the DG system design, challenges, and operation. The conclusions remarks are presented in the last section to finalize the paper.

2. DG Case Studies at World Universities

One of the best examples of a DG system on a university campus is at the University of California, San Diego (UCSD). The system has an installed capacity of 42 MW and meets 92% of the annual electricity demands of UCSD. An upgraded 22 kW prototype of a concentrated PV system is installed on the UCSD campus, including energy purchase agreements. This green university campus can be assumed to be an illustration of a “lab to market” model. UCSD has been further aiming to increase the utilization of PV production by integrating an energy storage system [10,11]. Another example of a DG system is located at the Illinois Institute of Technology (IIT). This system includes 4 MW gas turbine, wind turbines, and PV modules [12]. A DG case study at Princeton University consists of a 15 MW gas turbine and a 4.5 MW PV plant [13].

The DG system installed at Westlakes Campus of Central Lancashire University in England consists of a 5 kW wind turbine, a 20 kW PV system, a 21.6 kW heat pump, and a 6 kW solar thermal power system. For increasing renewable-based generation, enhancing

efficiency, and reducing the energy costs of the Lindow Building of the University of Central Lancashire at its Westlakes Campus, a microgrid system is operated [14]. At the campus of Genoa University in Italy, PV modules, a geothermal heat pump, thermal solar collectors, and a wind turbine on the rooftop of the faculty building are used for power generation. The total energy consumption and production of the centers are monitored in real time to be able to analyze the beneficial effects [15].

In addition to these universities, Hangzhou Dianzi University in China, the University of Nottingham in the UK, Chiang Mai Rajabhat University in Thailand, Technical University of Denmark, Berkeley Lab and New York University in the US have small and medium-scale capacity DG systems [16–20].

3. Overview of Hybrid Microgrid System

The proposed DG system is established in Marmara University, Faculty of Technology, Istanbul, Turkey. With this system, university researchers and academicians will be supported in the fields of fuel cell technologies, renewable energy systems, power electronics, sustainable energy management, energy managements systems, and hybrid power systems.

The aforementioned components of the DG system are shown in Figure 1 and are as follows: four pieces of PV panels (250 W) exist and create PV modules that are 1000 W rated power. A horizontal axis wind turbine has a 400 W output power with a permanent magnet synchronous machine (PMSM) as a generator. A PEMFC stack operates with a hydrogen generator (electrolyzer) with a 60 sL/h H₂ flow, which gives 1200 W output power. To provide H₂ to the stack, a low-pressure metal hydride hydrogen tank with 1500 sl is included. It should be mentioned that this stack is triggered by a fuel cell start-up battery with a 2 × 12 V output voltage and 120 Ah current capacity. This stack cabinet also has a 1500 W power-rated electronics load combined with it. A user-friendly interface is embedded into the PEMFC stack.

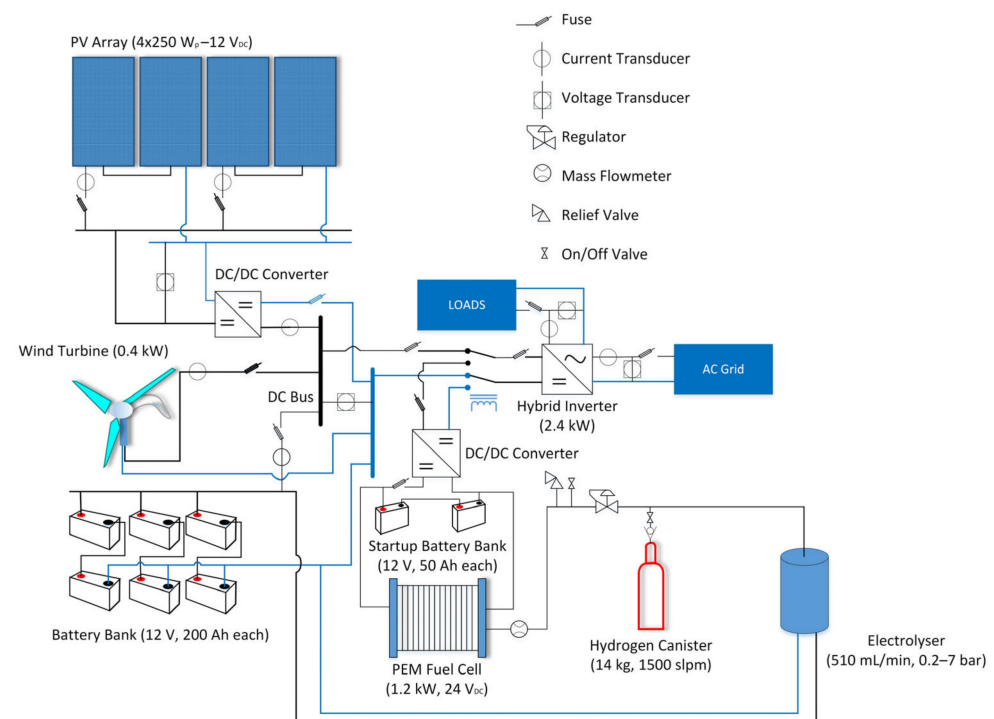


Figure 1. Overall system diagram.

All these DG elements are connected to the load side with a 2400 W-powered hybrid inverter. As a complementary power source, a battery bank contains six batteries, three connected in parallel and two in series, which are equal to 600 Ah current capacity, 24 V output voltage, and 14.4 kWh energy capacity. To operate the system to meet the desired

requirements, a central energy management unit is employed. This energy management system collects data for visualizing and controlling the power flow from the DG to the load side. This energy management system can be controlled by a user interface connected to the system.

The monitoring and control part of the DG system consists of two main parts: energy production and energy storage. The energy production units comprise a wind turbine, PV modules, and PEMFC system. The storage part consists of a battery bank, hydrogen canister, and electrolyzer. A Proton Exchange Membrane (PEM)-type hydrogen fuel cell is used as a backup energy generation system in this hybrid DG structure.

Since the polymer material is used as the electrolyte in the hydrogen fuel cell, these fuel cells are known as PEM cells. The electrodes used are carbon-structured. The most important feature of the PEMFC is that it has a membrane with proton conduction. The polymer membrane used is thin, small, and light. The most commonly used membrane material is Nafion[®], manufactured by DuPont (Wilmington, DE, USA). This membrane must be made of a material with high thermal, mechanical, and chemical resistance that is impermeable to water, fuel, oxygen, and other gases in the air. The wind turbine and PV modules on the rooftop of Marmara University, Faculty of Technology, are shown in Figure 2. The laboratory room with the wind turbine, PV modules, stack of hydrogen fuel cells, battery bank, electrolyzer, hydrogen canister (metal hydride tube), and other components is shown in Figure 3.



Figure 2. Wind turbine and PV modules on the rooftop of the faculty building.

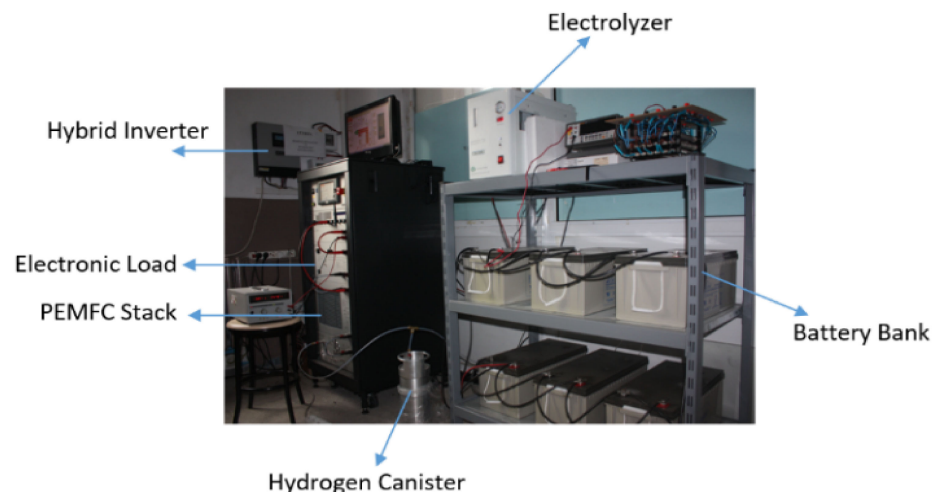


Figure 3. The DG system components.

The wind turbine specifications are given in Table 1.

Table 1. Wind Turbine Specifications.

| Specifications | Unit |
|--------------------|----------------------------|
| Nominal Power | 400 W |
| Swept Area | 1.07 m ² |
| Cut-in wind speed | 3.58 m/s |
| Cut-off wind speed | 49.2 m/s |
| Rotor diameter | 1.17 m |
| Alternator | Permanent Magnet Brushless |

The Weibull probability density function is generally used to calculate the energy generated from wind turbines, depending on the momentarily variable wind.

$$f(v) = \frac{k}{c} \left(\frac{v}{c}\right)^{k-1} \exp\left[-\left(\frac{v}{c}\right)^k\right] \tag{1}$$

where k is the shape parameter, and c is the scale parameter. In the case where much detail is known about the wind regime in a region, the k shape parameter can be set to 2. In this case, the Weibull probability density function is known as the Rayleigh probability density function [21].

$$f(v) = \frac{2v}{c^2} \exp\left[-\left(\frac{v}{c}\right)^2\right] \tag{2}$$

$$f(v) = \frac{\Pi v}{2\hat{v}^2} \exp\left[-\frac{\Pi}{4} \left(\frac{v}{\hat{v}}\right)^2\right] \tag{3}$$

where \hat{v} is an average wind speed in terms of m/s unit, denoted as 4.78 m/s.

According to the Weibull calculations, the wind turbine power curve can be expressed as in Figure 4. The total annual obtained energy from the wind turbine is calculated as 228.493 kWh, as seen in Table 2.

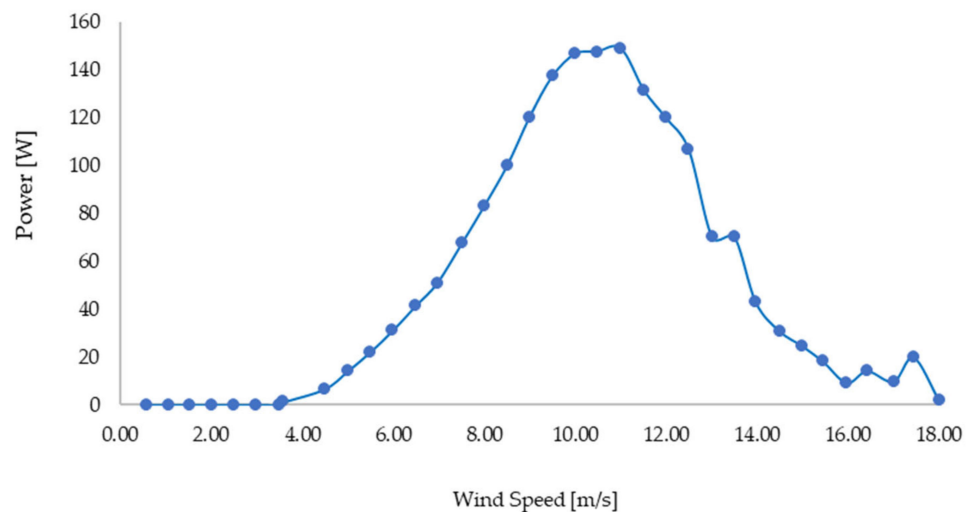


Figure 4. The DG system component (wind turbine).

Table 2. Rayleigh probability density functions and wind turbine calculations.

| Wind Speed [m/s] | Power [W] | $f(v)$ | Hours/Year at v | Energy [Wh/Year] |
|------------------|-----------|-----------|-------------------|------------------|
| 1.06 | 0 | 0.065 | 569.4 | 0 |
| 2.02 | 0 | 0.1194 | 1045.944 | 0 |
| 2.99 | 0 | 0.1512 | 1324.512 | 0 |
| 3.58 | 1 | 0.1581 | 1384.956 | 1620.39852 |
| 5.00 | 14 | 0.1453 | 1272.828 | 17,921.41824 |
| 5.99 | 31 | 0.1196 | 1047.696 | 32,499.52992 |
| 6.97 | 51 | 0.0893 | 782.268 | 39,848.73192 |
| 8.00 | 83 | 0.0609 | 533.484 | 44,311.18104 |
| 9.00 | 120 | 0.0382 | 334.632 | 40,232.80536 |
| 10.00 | 146 | 0.0221 | 193.596 | 28,357.94208 |
| 11.00 | 149 | 0.0118 | 103.368 | 15,372.88896 |
| 11.99 | 120 | 0.00585 | 51.246 | 6140.80818 |
| 13.01 | 70 | 0.00268 | 23.4768 | 1643.376 |
| 13.97 | 43 | 0.00114 | 9.9864 | 427.817376 |
| 14.99 | 25 | 0.000452 | 3.95952 | 97.4833824 |
| 15.97 | 9 | 0.000166 | 1.45416 | 13.5091464 |
| 17.00 | 10 | 0.0000569 | 0.498444 | 4.8847512 |
| 18.00 | 2 | 0.000018 | 0.15768 | 0.3169368 |
| | | | Total | 228,493.0918 |

The parameters of the PV module are reported in Table 3. With regards to geographic location, the coordinates of the aforementioned system are located at 40°59' North Latitude, 29°3' East Longitude.

$$\delta = 23,45 \sin \left[\frac{360}{365} (n - 81) \right] \tag{4}$$

$$\beta_A = 90 - L + \delta \tag{5}$$

$$PV_{tilt} = 90 - \beta_A \tag{6}$$

where δ is the solar declination angle, and β_A is an altitude angle (the altitude angle is the angle between the sun and the local horizon directly beneath the sun), PV_{tilt} is the optimum PV module tilt angle, fixed at 30°, L is the latitude of the site, and n is number of days.

$$I_{total} = I_{beam} + I_{diffuse} + I_{reflected} \tag{7}$$

$$I_{beam} = I_{BH} R_B \tag{8}$$

$$I_{BH} = I_H - I_{DH} \tag{9}$$

$$H_{SR} = \cos^{-1}(-\tan L \tan \delta) \tag{10}$$

$$H_{SRC} = \min \left\{ \cos^{-1}(-\tan L \tan \delta), \cos^{-1}[-\tan L(L - PV_{tilt}) \tan \delta] \right\} \tag{11}$$

$$R_B = \frac{\cos(L - PV_{tilt}) \cos \delta \sin H_{SRC} + H_{SRC} \sin(L - PV_{tilt}) \sin \delta}{\cos L \cos \delta \sin H_{SR} + H_{SR} \sin L \sin \delta} \tag{12}$$

$$C = \frac{I_H}{I_O} \tag{13}$$

$$\frac{I_{DH}}{I_H} = 1.390 - 4.207C + 5.531C^2 - 3.108C^3 \tag{14}$$

$$I_{diffuse} = I_{DH} \left(\frac{1 + \cos(PV_{tilt})}{2} \right) \tag{15}$$

$$I_O = \left(\frac{24}{\pi} \right) SC \left[1 + 0.034 \cos \left(\frac{360n}{365} \right) \right] (\cos L \cos \delta \sin H_{SR} + H_{SR} \sin L \sin \delta) \tag{16}$$

$$I_{reflected} = \rho I_H \left(\frac{1 - \cos(PV_{tilt})}{2} \right) \tag{17}$$

where I_{total} is the total daily solar irradiance on the PV module, I_{beam} is the beam solar irradiance on the PV module, $I_{diffuse}$ is the diffuse solar irradiance on the PV module, $I_{reflected}$ is the reflected solar radiation on the PV module, I_H is the total average daily horizontal solar irradiance, I_{BH} is the beam irradiance on the horizontal surface, R_B is the beam tilt factor, H_{SRC} is the sunrise hour angle for the collector (when the sun first strikes the collector face, $\theta = 90^\circ$), H_{SR} is the sunrise hour angle (in radians), C is the clearness index, I_0 is extraterrestrial insolation on a horizontal surface at the site, I_H is insolation on a horizontal surface, and ρ is ground reflectivity. The total solar irradiance profile is shown in Figure 5.

Table 3. PV module (polycrystalline cells) specifications.

| Features | Values (UOM) |
|-----------------------------|--------------------|
| Module Efficiency (%) | 15.71 |
| Cell Efficiency (%) | 17.9 |
| Peak Power (P) | 250 Wp |
| Max Power Voltage (Vmp) | 30.6 V |
| Max Power Current (Imp) | 8.17 A |
| Open-Circuit Voltage (Voc) | 38 V |
| Short-Circuit Current (Isc) | 8.71 A |
| Number of Cells | 60 |
| Dimensions | 1640 × 990 × 35 mm |

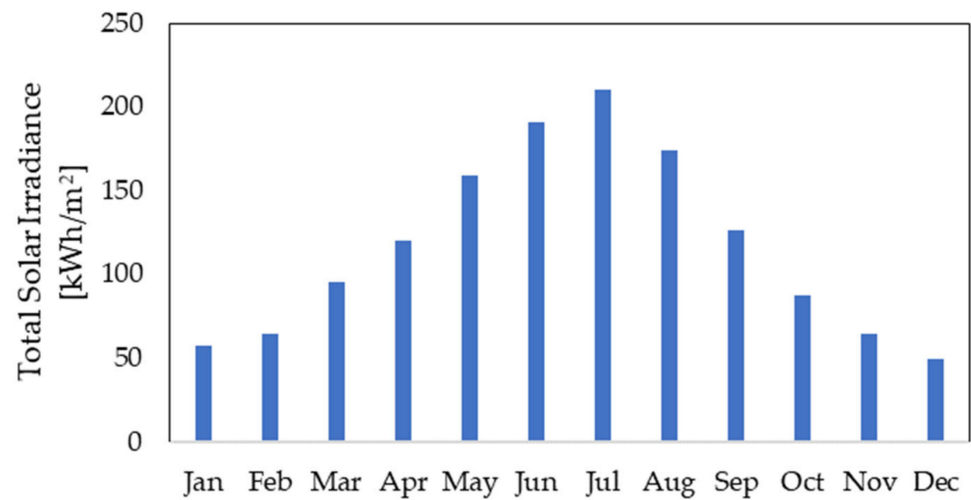


Figure 5. Monthly solar irradiance.

To be aware of the potential of the faculty’s location, the 3D Sun-Path program was used to assist in comparing solar altitude, azimuth angles, and zenith angles [22]. The program interface is shown in Figure 6.

$$E_{total} = A_{module} \eta_{module} I_{total} PR \tag{18}$$

where E_{total} is the produced total PV output energy (kWh), PR is the performance ratio (0.5~0.9), A_{module} is the module area (m²), and η_{module} is the module efficiency (%).

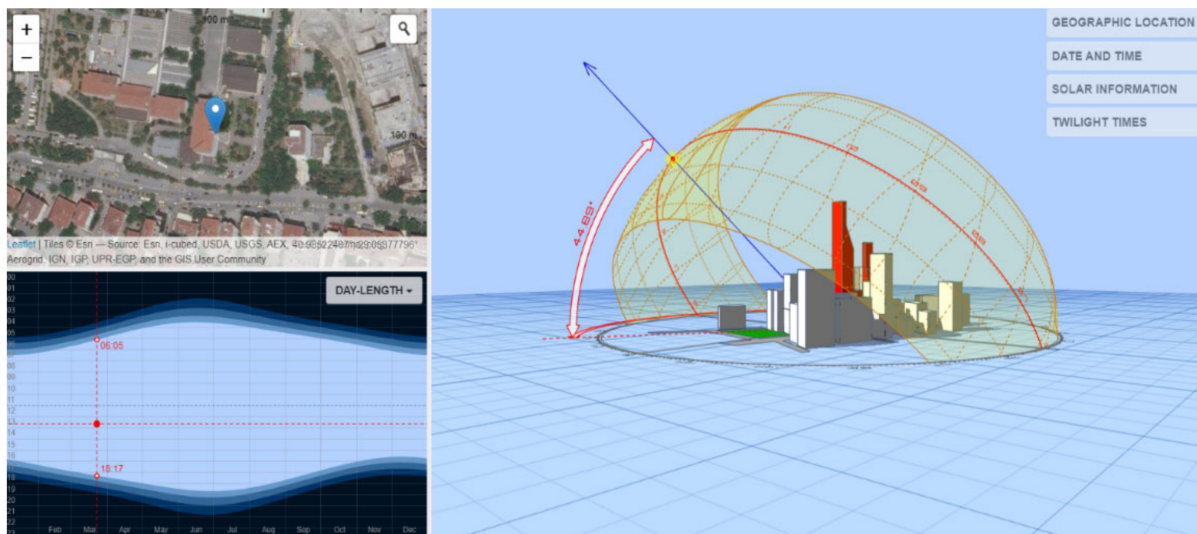


Figure 6. Geographic location of the faculty building and solar positions.

Equation (18) expresses the total annual produced PV energy. By this calculation, the annual average produced energy profile is plotted and illustrated in Figure 7; the total annual PV energy corresponds to 1335.05 kWh. Figure 8 depicts the hourly total produced PV output energy. It can be extracted that generation is higher at noon than at the other times.

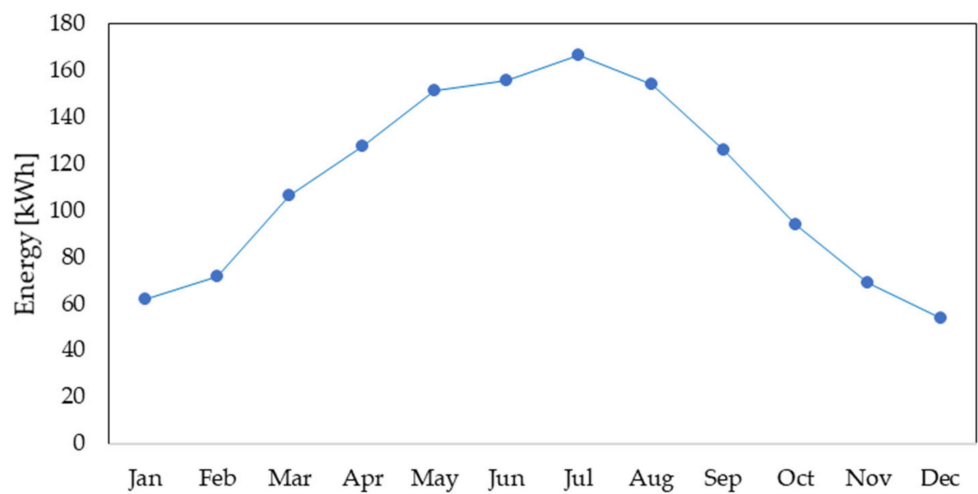


Figure 7. Total produced PV output energy.

The system is established and designed to operate both independently and connected to the grid. The system can be fed by the utility grid, with the aim of hybrid inverter operation when the state of charge (SoC) of battery bank is lower than desired level, as this means the stored energy is not able to meet the load demand. When the battery bank meets the load requirement, the system continues to operate independently of the grid. This energy management scenario in these DG systems ensures the flexibility and sustainability of the systems.

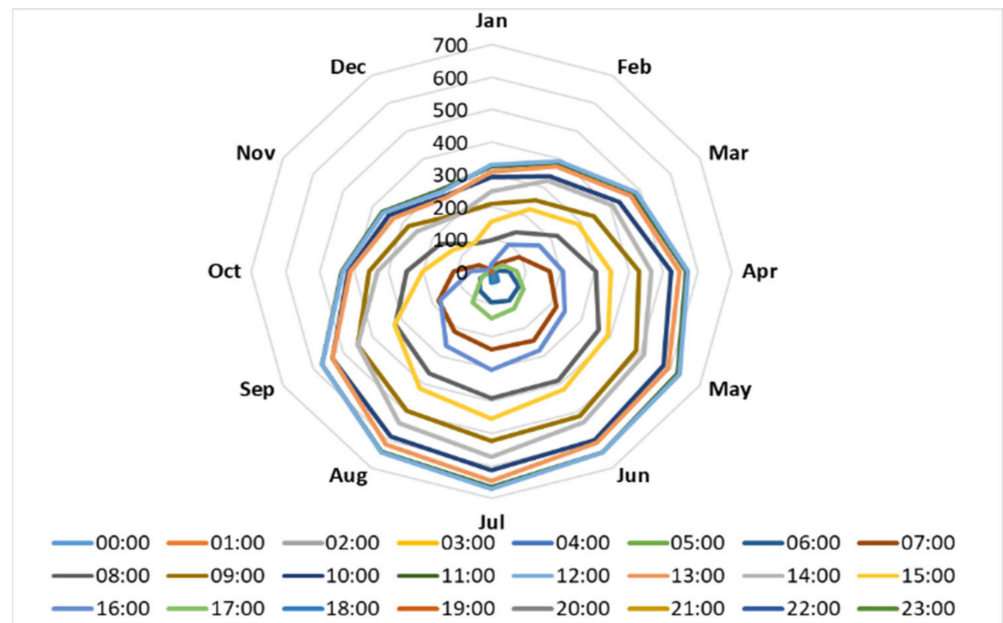


Figure 8. Total produced hourly PV output energy (kWh).

As seen in Table 4, the daily energy requirement was calculated as 14,360 kWh. In this case, the annual average energy demand is 3791.04 kWh. Since the total annual energy demand is 3791.04 kWh, the 2029.497 kWh of energy that cannot be met by production can be supplied from the grid via the hybrid inverter.

$$Ah = \frac{nkE_{demand}}{v_{DC}DoD} \tag{19}$$

where n represents days of autonomy ($n = 2$), DoD is the maximum depth of discharge ($DoD = 40\%$), v_{DC} is DC bus voltage ($v_{DC} = 24\text{ V}$), E_{demand} is total energy demand, k is the temperature correction factor ($k = 1.04$). Six batteries of 120 Ah each are connected in series and parallel as shown in Figure 2 to obtain nominal 24 V and a total power of 14.4 kWh. The system components are installed in the “Renewable Energy Laboratory” within the Faculty. The lighting and the “plug and play” loads are connected to the DG system. The lighting (armature) loads are shown in Figure 9.

Table 4. The load profile of the laboratory.

| Loads | # | Nominal Power [W] | Hours of Use/Day | Energy Use/Day [Wh/Day] |
|------------------|----|-------------------|------------------|-------------------------|
| Air Conditioning | 1 | 560 | 5 * | 2800 |
| Electrolyzer | 1 | 400 | 2 | 800 |
| Lighting | 12 | 48 | 10 * | 5.760 |
| PC | 2 | 250 | 10 | 5000 |
| Total | | 2.616 | | 14,360 |

* Discrete time.



Figure 9. The lighting loads in the laboratory.

The annual average energy produced from the wind turbine and PV modules is 1563.543 kWh. The PEMFC can generate 198 kWh of energy per year when we estimate that it produces 3 h of average power per day. In this case, the total energy produced from the hybrid microgrid is 1761.543 kWh. By means of the electrolyzer in the system, the hydrogen demand of the hydrogen fuel cell stack can be met. The hydrogen produced by the electrolyzer is stored in the metal hydride canister. The charge pressure of the metal hydride canister is 5 bar, and the discharge pressure is 2–5 bar. The weight is 14 kg, and the capacity is 1500 lt. The empty canister can be fully filled in 50 h. A PEM-type hydrogen fuel cell stack is used in the system. The stack in the system can run for 8 h with a full hydrogen canister at a 250 W average. In order for the hydrogen fuel cell stack to operate at a maximum power of 1200 W, it should be supplied with 13 L of hydrogen per minute. The output flow of the electrolyzer used in the system is 510 mL per minute. Therefore, the produced hydrogen should be stored in order for the heap to operate at a power of 300 W.

A Graphical User Interface (GUI) is used for the hydrogen fuel cell stack used in the system, as shown in Figure 10. With the help of this interface, all inputs and outputs of the system can be monitored and controlled in real time. This GUI is a helpful interface that can also be used for education purposes, such as in post-graduate courses, to boost awareness of this topic. It enables us to try different power electronic connection scenarios for the output.

Additionally, polarization curves of fuel cells for different load characteristics, determination of charge-discharge characteristics of batteries, energy conversion and efficiency analysis, and wind turbine and PV module data were obtained. The input power of the system, the powers used, and the energy losses are shown in a Sankey diagram. This diagram also shows the state of charge of the start-up batteries of the fuel cell stack, as can be seen in Figure 10. The most important parameter of a hydrogen fuel cell is the polarization curve. The polarization curve is a graph showing the change in current of a fuel cell or stack, depending on voltage or power. This curve determines the performance of the cell. Through the GUI, it is possible to monitor the instantaneous polarization curve of the PEMFC Stack, as shown in Figure 11. The GUI of the PEMFC facilitates data acquisition relevant to all variables, as seen in Figure 12.

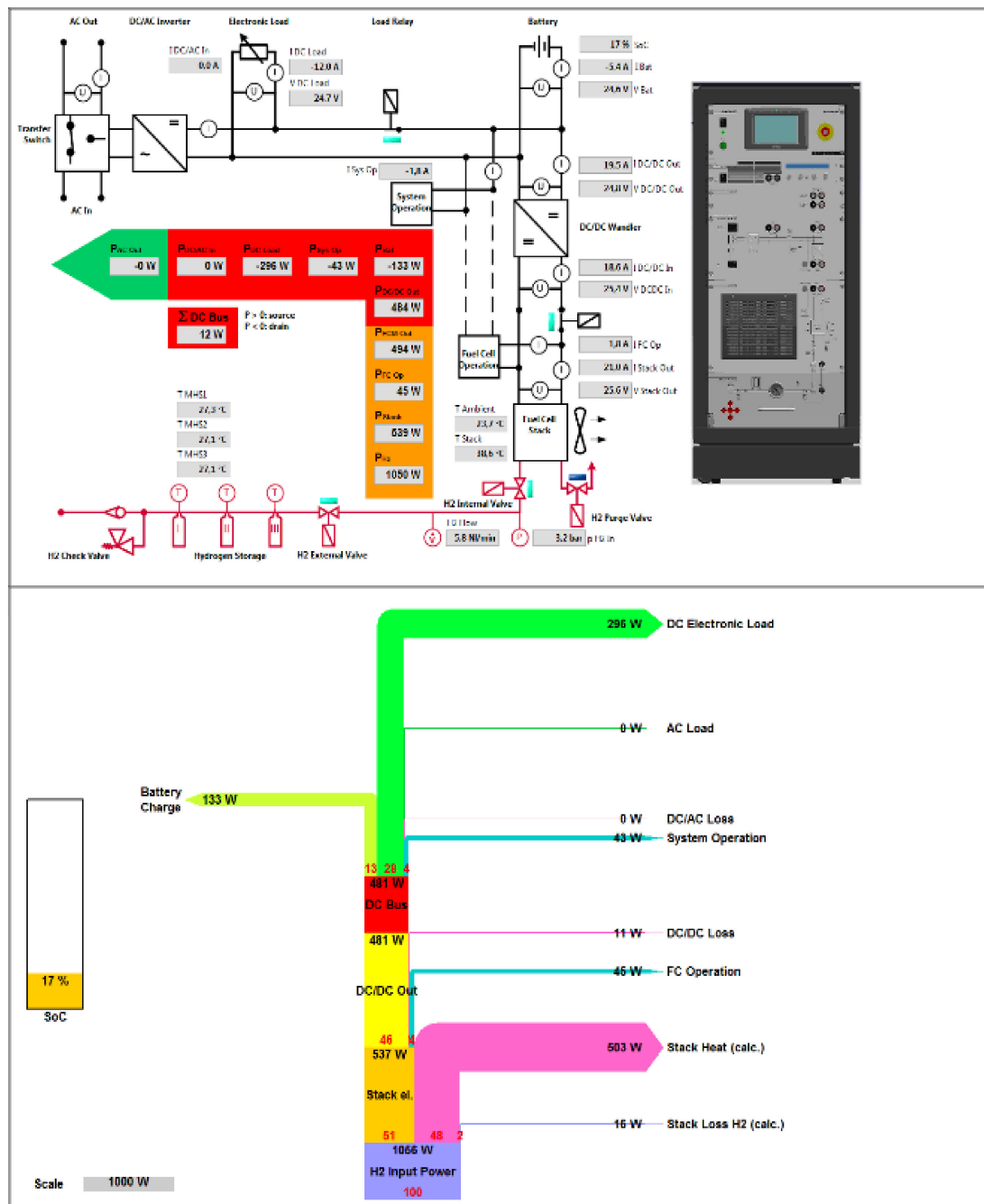


Figure 10. GUI of PEMFC Stack, Components, and Sankey diagram.

Figure 13 shows the voltage, current, power and temperature curves of the collected PEMFC stack for approximately one hour (4000 s). The data for the SoC level of the start-up battery and the PEMFC’s DC/DC converter output voltages are shown in Figure 14.

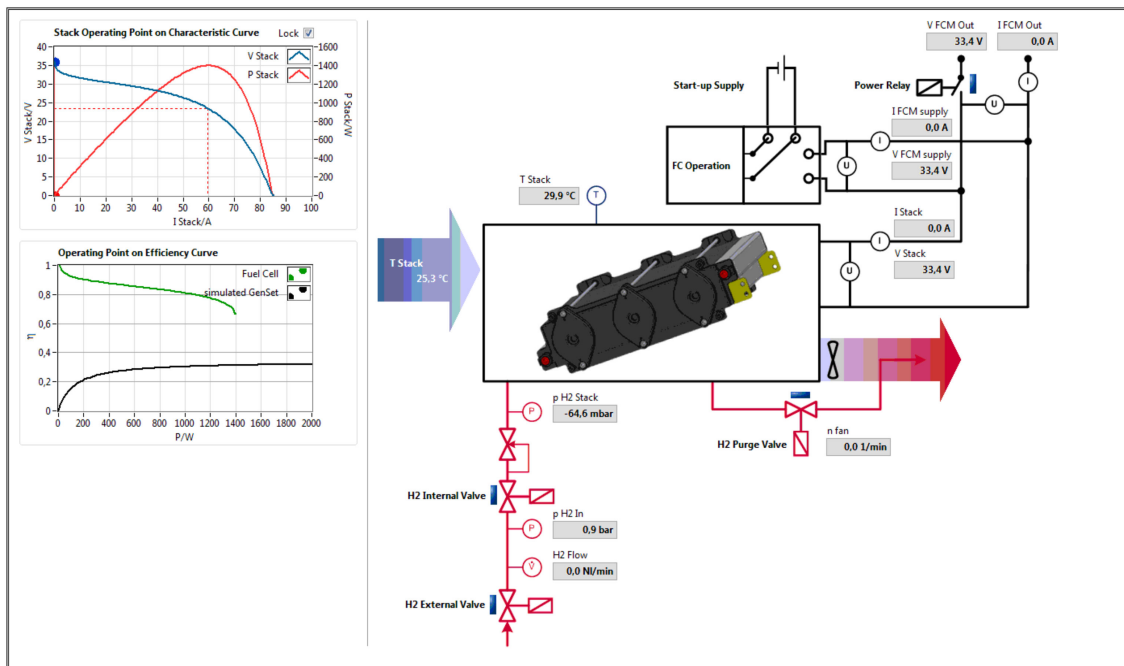


Figure 11. The Polarization Curves of the PEMFC.

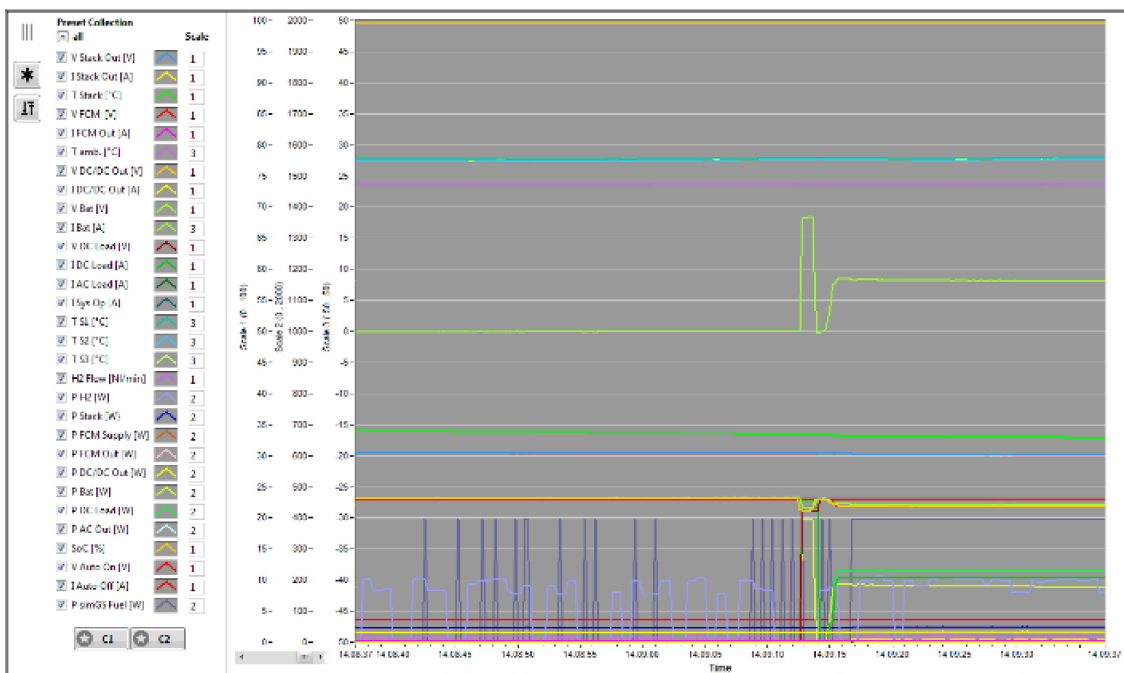


Figure 12. Data acquisition screen.

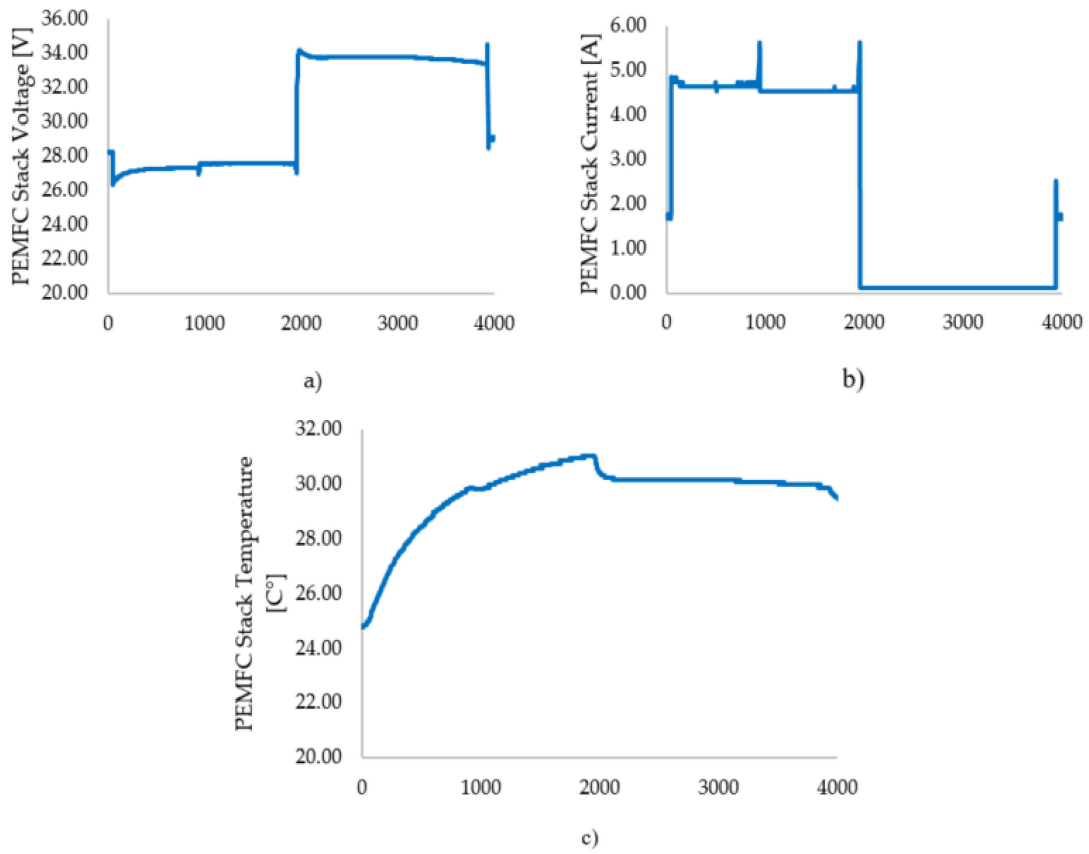


Figure 13. (a) PEMFC stack voltage, (b) PEMFC stack current, and (c) PEMFC stack temperature (C°).

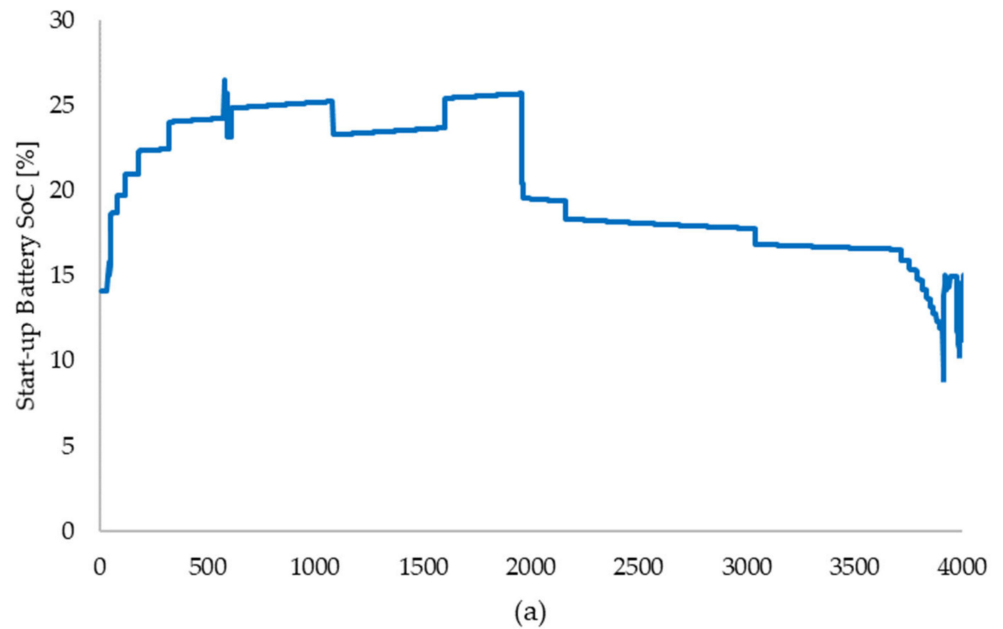


Figure 14. Cont.

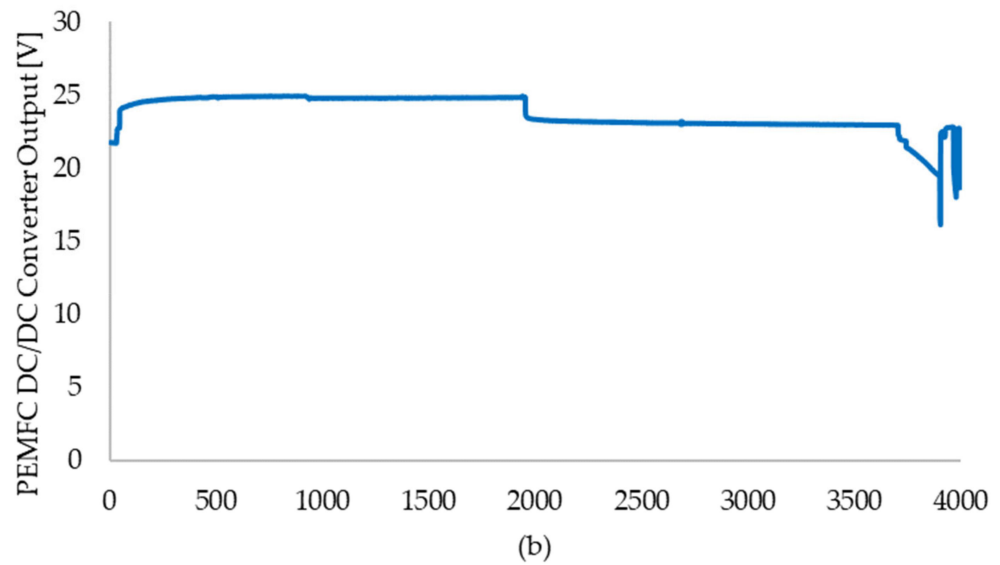


Figure 14. (a) Start-up battery SoC levels; (b) PEMFC's DC/DC converter output voltages.

4. Operation Results

The PEMFC-based grid-connected DG system at Marmara University, Faculty of Technology, was analyzed in detail in this study. It was found that 53.53% of the total energy demand was met by the utility grid, while 46.47% of the demand was met by the DG system, as can be seen in Figure 15. As seen in Table 4, the annual average energy demand was calculated as 3791.04 kWh; 2029.497 kWh that could not be met by production could be supplied from the grid via the hybrid inverter. The remaining energy demand was met by the distributed generation, 1761.543 kWh. To this end, we can clarify that 53.53% of the total energy demand is met by the utility grid, while 46.47% of the demand is met by the DG system.

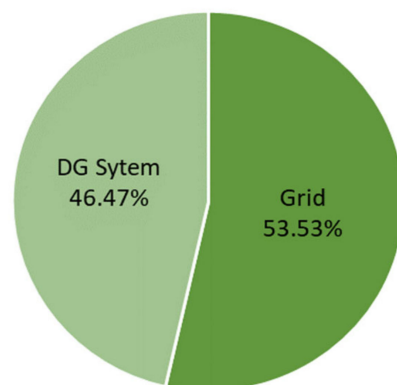


Figure 15. Grid support and DG energy production.

Energy supplied from the utility grid, production of DG systems, and energy demands for the system are given in Table 5. With respect to the energy values of DGs in kWh, most of the demands are met by PV, 35.22% of total production, i.e., nearly 76% of the DG system, as can be seen in Figure 16. The contributions of the wind and PEMFC, (nearly 24% of the DG system) are similar in percentage at 6.02% and 5.23%, respectively.

Table 5. The DG and energy demands (kWh).

| E_{Wind} | E_{PV} | E_{PEMFC} | $E_{DG} = E_{Wind} + E_{PV} + E_{PEMFC}$ | E_{grid} | E_{demand} |
|------------|----------|-------------|--|------------|--------------|
| 228.493 | 1335.050 | 198 | 1761.453 | 2029.497 | 3791.040 |

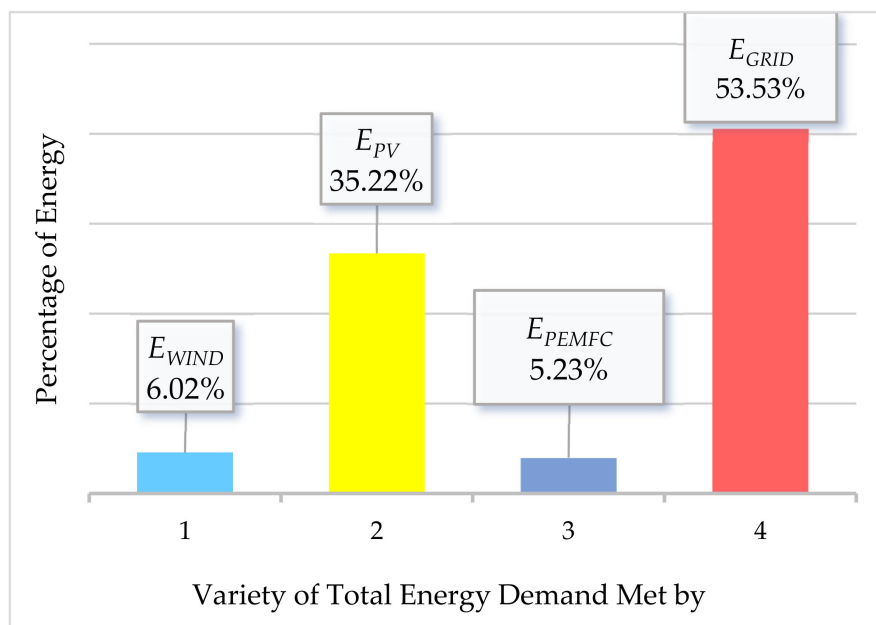


Figure 16. The pie chart of power generation and grid support rates of the microgrid for a defined operation.

5. Conclusions

The results and analysis were realized under transient and steady-state conditions. According to the results of the performance analysis, the important points to highlight in order to assist researchers working in this field are as follows. First, it can be extracted that the PV modules are more useful and efficient in urban applications than wind turbines. For example, we see barely 160 W produced by the wind turbine, with a nominal 400 W of power used in this system. The most important reason for this is that the wind turbines installed in places where there are many buildings cannot catch the necessary wind due to its dynamic nature. Another important consequence of the DG system is that the hydrogen required by the fuel cell is supplied by the electrolyzer, which is supplied from renewable energy instead of ready hydrogen tanks. However, the PEM-type fuel cell stack is not suitable for continuous operation if the electrolyzer has a low hydrogen-producing capacity. Although the nominal power of the fuel cell is 1200 W, it is operated with 250 W output power. The energy required for the operation of the electrolyzer is produced entirely from renewable energy. With the increase of the power and size of the electrolyzer, PEMFC’s support for the DG system will increase even more.

The key components of the system are power switching and power electronics components. The frequency of the power switching elements of the inverter used in the system during connection and disconnection from the grid affects the loads in the system. This particularly affects fluorescent lights, which operate with a gas discharge.

Author Contributions: A.N.A. and E.D. wrote the manuscript. E.D. performed the experimental design of the microgrid and data acquisition. A.N.A. operated the system. A.N.A., E.D. and Y.Y. gathered and evaluated the results. A.N.A., E.D. and Y.Y. reviewed the manuscript. All authors have read and agreed to the published version of the manuscript.

Funding: This study was supported by grant from Scientific Research Projects Unit (BAPKO) project number: FEN-E-120314-0069.

Institutional Review Board Statement: Not applicable.

Informed Consent Statement: Not applicable.

Data Availability Statement: Not applicable; however, the data may be requested by reaching out to the authors through email.

Conflicts of Interest: The authors declare no conflict of interest.

References

1. About Microgrids, Microgrids at Berkeley Lab. Available online: <https://building-microgrid.lbl.gov/about-microgrids> (accessed on 15 May 2020).
2. Unamuno, E.; Barrena, J.A. Hybrid AC/DC microgrids—Part I: Review and classification of topologies. *Renew. Sustain. Energy Rev.* **2015**, *52*, 1251–1259. [CrossRef]
3. U.S. Department of Energy. Distributed Energy. Available online: <http://energy.gov/oe/technology-development/smart-grid/distributed-energy> (accessed on 16 May 2020).
4. Guo, L.; Vengalil, M.; Abdul, N.M.M.; Wang, K. Design and implementation of virtual laboratory for a microgrid with renewable energy sources. *Comput. Appl. Eng. Educ.* **2021**, *30*, 349–361. [CrossRef]
5. Zuo, G.; Dou, Y.; Chang, X.; Chen, Y. Design and Application of a Standalone Hybrid Wind–Solar System for Automatic Observation Systems Used in the Polar Region. *Appl. Sci.* **2018**, *8*, 2376. [CrossRef]
6. Beccali, M.; Bonomolo, M.; Di Pietra, B.; Leone, G.; Martorana, F. Solar and Heat Pump Systems for Domestic Hot Water Production on a Small Island: The Case Study of Lampedusa. *Appl. Sci.* **2020**, *10*, 5968. [CrossRef]
7. Akpolat, A.N.; Yang, Y.; Blaabjerg, F.; Dursun, E.; Kuzucuoglu, A.E. Design implementation and operation of an education laboratory-scale microgrid. *IEEE Access* **2021**, *9*, 57949–57966. [CrossRef]
8. Reis, G.L.; Brando, D.L.; Oliveira, J.H.; Araujo, L.S.; Filho, B.J.C. Case Study of Single-Controllable Microgrid: A Practical Implementation. *Energies* **2022**, *15*, 6400. [CrossRef]
9. Sun, C.; Leto, S. A novel joint bidding technique for fuel cell wind turbine photovoltaic storage unit and demand response considering prediction models analysis Effect's. *Int. J. Hydrogen Energy* **2020**, *45*, 6823–6837. [CrossRef]
10. Han, Y.; Chen, W.; Li, Q.; Yang, H.; Zare, F.; Zheng, Y. Two-level energy management strategy for PV-Fuel cell-battery-based DC microgrid. *Int. J. Hydrogen Energy* **2019**, *44*, 19395–19404. [CrossRef]
11. Washom, B.; Dilliot, J.; Weil, D.; Kleissl, J.; Balac, N.; Torre, W.; Richter, C. Ivory Tower of Power: Microgrid Implementation at the University of California, San Diego. *IEEE Power Energy Mag.* **2013**, *11*, 28–32. [CrossRef]
12. Liang, C.; Shahidehpour, M. DC Microgrids: Economic Operation and Enhancement of Resilience by Hierarchical Control. *IEEE T Smart Grid* **2014**, *5*, 2517–2526. [CrossRef]
13. Case Study: Microgrid at Princeton University, Consulting-Specifying Engineer. 2015. Available online: <http://www.csemag.com/single-article/case-study-microgrid-at-princetonuniversity/a852c6c36420f738c8ecf66de7aa3dd1.html> (accessed on 20 May 2020).
14. The University of Central Lancashire (UCLAN). Available online: http://www.uclan.ac.uk/courses/msc_pgddip_renewable_energy_engineering.php (accessed on 20 May 2020).
15. Bracco, S.; Delfino, F.; Pampararo, F.; Robba, M.; Rossi, M. Planning and management of sustainable microgrids: The test-bed facilities at the University of Genoa. In *Proceedings of the Africon Conference; Pointe aux Piments, Mauritius, 9–12 September 2013*, pp. 1–5. [CrossRef]
16. The Microgrids Group at Berkeley Lab, “Examples of Microgrids”, Berkeley Lab. 2019. Available online: <https://building-microgrid.lbl.gov/examples-microgrids> (accessed on 20 May 2020).
17. Davies, R.; Sumner, M.; Christopher, E. Energy storage control for a small community microgrid. In Proceedings of the 7th IET International Conference on Power Electronics, Machines and Drives (PEMD 2014), Manchester, UK, 8–10 April 2014. [CrossRef]
18. Setthapun, W.; Srikaew, S.; Rakwichian, J.; Tantranont, N.; Rakwichian, W.; Singh, R. The integration and transition to a DC based community: A case study of the Smart Community in Chiang Mai World Green City. In Proceedings of the First International Conference on DC Microgrids (ICDCM), Atlanta, GA, USA, 7–10 June 2015; pp. 205–209. [CrossRef]
19. Mihet-Popa, L.; Groza, V.; Isleifsson, F. Experimental testing for stability analysis of distributed energy resources components with storage devices and loads. In Proceedings of the International Instrumentation and Measurement Technology Conference Proceedings, Graz, Austria, 13–16 May 2012; pp. 588–593. [CrossRef]
20. Akpolat, A.N.; Dursun, E. ‘From microgrid to smart grid: A review of campus projects. In Proceedings of the International Engineering, Science and Education Conference, Diyarbakir, Turkey, 1–3 December 2016; pp. 379–387.

21. Masters, G.M. *Renewable and Efficient Electric Power Systems*; Wiley: Hoboken, NJ, USA, 2014.
22. Marsh, A. 3D Sun-Path. Available online: <https://drajmarsh.bitbucket.io/sunpath3d.html> (accessed on 1 June 2020).

Disclaimer/Publisher's Note: The statements, opinions and data contained in all publications are solely those of the individual author(s) and contributor(s) and not of MDPI and/or the editor(s). MDPI and/or the editor(s) disclaim responsibility for any injury to people or property resulting from any ideas, methods, instructions or products referred to in the content.